Search for high T_c in layered structures: The case of LiB

Matteo Calandra
Institut de Minéralogie et de Physique des Milieux condensés, case 115, 4 place Jussieu, 75252, Paris cedex 05, France

Aleksey N. Kolmogorov and Stefano Curtarolo
Department of Mechanical Engineering and Material Science, Duke University, Durham, North Carolina 27708, USA
(Received 19 December 2006; published 16 April 2007)

Using electronic structure calculation we study the superconducting properties of the theoretically devised superconductor MS1-LiB (LiB). We calculate the electron-phonon coupling ($\lambda=0.62$) and the phonon frequency logarithmic average ($\langle\omega\rangle_{\log}=54.6$ meV) and show that the LiB critical temperature is in the range of 10–15 K, despite the frozen-phonon deformation potential being of the same order of MgB_2. As a consequence, LiB captures some of the essential physics of MgB_2 but (i) the electron-phonon coupling due to σ states is smaller and (ii) the precious contribution of the π carriers to the critical temperature is lacking. We investigate the possible change in T_c that can be induced by doping and pressure and find that these conditions cannot easily increase T_c in LiB.

DOI: 10.1103/PhysRevB.75.144506 PACS number(s): 74.70.Ad, 63.20.Kr, 63.20.Dj, 78.30.Er

I. INTRODUCTION

The quest for superconductivity in layered structures has become the focus of intense research since the discovery of superconductivity in MgB_2 ($T_c=39$ K).[1] The layered structure of MgB_2 generates one of its most prominent features, namely, the B $2p_{xy}$ orbitals form σ bands[2–4] which are weakly dispersing along the k_z direction and have a marked two dimensional character. In MgB_2 the σ bands are hole doped, but the top of these bands is only $\approx$0.5 eV higher than the Fermi level. The σ bands Fermi surface sheets,[4] two slightly warped cylinders with axis perpendicular to the boron layers, generate a huge electron-phonon coupling along the k_z direction. The carriers in the π bands, formed by the B $2p_z$ orbitals, further enhance the average electron-phonon coupling.[5]

The formation of σ and π states is typical of graphitelike structures composed by boron or carbon atoms. Given the success of MgB_2 it is natural to look for high-T_c superconductivity in structures having similar features. The problem is that, given the boron layers, small variations in the valence or mass of the intercalant or in the structural parameters are sufficient to considerably alter the σ or π bands positions or the shape of their Fermi surfaces and consequently destroy superconductivity. For one or some of these reasons AlB_2, ZrB_2, NbB_2, MoB_2, YB_2, TaB_2, TiB_2, HfB_2, VB_2, and CrB_2 are not superconducting.[6–8]

The hope of finding new superconducting materials in layered structures was recently increased by the discovery of superconductivity in the graphite intercalated compounds, YbC_6 and CaC_6.[9,10] This is particularly promising since a huge number of intercalants are available for graphite.[11] In CaC_6, despite the layered structure and the existence of σ and π bands originated from the carbon $2p$ orbitals, the electronic structure close to the Fermi level is completely different from that of MgB_2. The π bands, reminiscent of the graphite ones, and an intercalant free-electron-like band[12,13] cross the Fermi energy. The intercalant band forms a spherical Fermi surface.[14,15] The electron-phonon coupling of CaC_6 ($\lambda=0.83$) is mainly due to coupling of the interlayer band with C vibrations perpendicular to the graphite layers and with Ca vibrations. So, even though missing the σ-bands, CaC_6 reaches an interesting 11.5 K T_c. This temperature is substantially enhanced by pressure [$T_c=15.1$ K at $\approx$8 GPa (Ref. 16)], contrary to what happens in MgB_2.

As can be seen from the above examples, even if one restricts to sandwich structures formed by boron or carbon layers, the details of the electronic and phonon spectra and, subsequently, the critical temperature can change dramatically when the intercalant is included. As a consequence, a theoretical approach is absolutely necessary to identify the most probable superconductors or at least to exclude the less probable ones.

An attempt in this direction has been recently made in Ref. 17, where by using *ab initio* methods the authors studied the possible hole doping of LiBC, a $\approx$1 eV gap semiconductor. The authors suggested that a T_c of the order of MgB_2 could be reached if the insulating LiBC is substantially doped with holes to obtain $Li_{0.5}BC$. Successive experimental studies have indicated that the structural response to the introduction of holes unfavorably modifies the electronic structure of Li_xBC, and so far no high-T_c superconductivity has been found in this system.[18,19]

Ideally designing new superconductors *ab initio* requires three steps. The first is the determination of the most stable structures given a set of atomic species. The second is the calculation of the electronic structure to verify that the given structure is at least metallic or can be made metallic easily. The third is the determination of the phonon dispersion and of the electron-phonon parameters.

The first point is a daunting task even if one restricts one's search to a specific set of likely candidates.[20,21] A systematic approach to tackle this problem has been recently offered in the way of data mining of *ab initio* calculations.[22–24] In this method one uses the informations obtained from *ab initio* calculations of many different structures to build a database that can be then used to judge the stability of new structures. Application of this method to intermetallics has led to the

identification of new layered lithium monoboride phases which have a good chance to form under proper synthesis conditions.[25]

Once a stable metallic structure is given, a calculation of the phonon spectra and of the electron-phonon coupling needs to be performed to obtain T_c. Indeed, while some qualitative information can be extracted from electronic structure,[2] for a quantitative analysis step three is absolutely necessary.

In this work we investigate the superconducting properties of the previously determined metal sandwich (MS) lithium monoboride[25] by calculating its phonon spectrum and electron-phonon parameters. This system is metallic and, from qualitative arguments, one can infer that T_c is of the same order of that of MgB_2.[25] Indeed this system has an electronic structure which is a hybrid between those of MgB_2 and CaC_6, since there are hole-doped σ bands forming cylindrical Fermi surfaces and there is an intercalant band crossing the Fermi level. Moreover the deformation potential is comparable to that of MgB_2.[25] From this point of view, LiB is a much more promising material than $Li_{0.5}BC$, because even without doping it has a significant density of σ states at the Fermi level.

Unfortunately, the full electron-phonon coupling calculations performed in this paper indicate that LiB should have a T_c in a 10–15 K range. We show that LiB captures some of the important physics of MgB_2, namely the role of the σ bands, but it lacks the contribution of the π states to the electron-phonon coupling and it is only a far relative of CaC_6 because the interlayer band is very weakly coupled with the phonons. In an attempt to improve the situation we examine what role the hydrostatic pressure and doping can play in determining the critical temperature.

II. TECHNICAL DETAILS

In all our calculations of the layered lithium monoboride we have used the MS1 theoretical crystal structure basing our choice on the following considerations. On the one hand, it has the smallest unit cell of all MS structures, which offers computational efficiency. On the other hand, even though other stacking sequences are possible (e.g., MS2, Refs. 25 and 26), MS1 is a good representative model of the layered lithium monoboride because the long-period shifts are expected to have little effect on its superconducting properties.[27] MS1-LiB has a rhombohedral unit cell with $R\bar{3}m$ space group. There are four atoms in the primitive unit cell with Wyckoff positions $\mathrm{Li}(2c)(1/2-z_{\mathrm{Li}},1/2-z_{\mathrm{Li}},1/2-z_{\mathrm{Li}})$, $\mathrm{Li}(2c)(1/6+z_{\mathrm{Li}},1/6+z_{\mathrm{Li}},1/6+z_{\mathrm{Li}})$, $\mathrm{B}(2c)(-\delta,-\delta,-\delta)$, and $\mathrm{B}(2c)(2/3-\delta,2/3-\delta,2/3-\delta)$. The fully relaxed parameters are $a=b=c=5.92$ Å, $\alpha=\beta=\gamma=29.8^{\circ}$.

Density functional theory (DFT) calculations are performed using the Quantum ESPRESSO package[28] within the generalized gradient approximation (GGA).[29] We use norm-conserving pseudopotentials[30] with configuration $2s^12p^0$ and nonlinear core correction[31] for Li, and configuration $2s^22p^1$ for B. The wave functions are expanded using a 50 Ry cutoff. The dynamical matrices and the electron-phonon coupling are calculated using density functional perturbation theory in the linear response.[28] For the electronic integration in the phonon calculation we use an $N_k=12\times12\times12$ uniform **k**-point mesh and Hermite-Gaussian smearing from 0.05 Ry. For the evaluation of the electron-phonon coupling we use an $N_k=40\times40\times40$ Monkhorst-Pack mesh. For the λ average over the phonon momentum **q** we use an $N_q=4\times4\times4$ **q**-point mesh. The phonon dispersion is obtained by Fourier interpolation of the dynamical matrices computed on the N_q mesh.

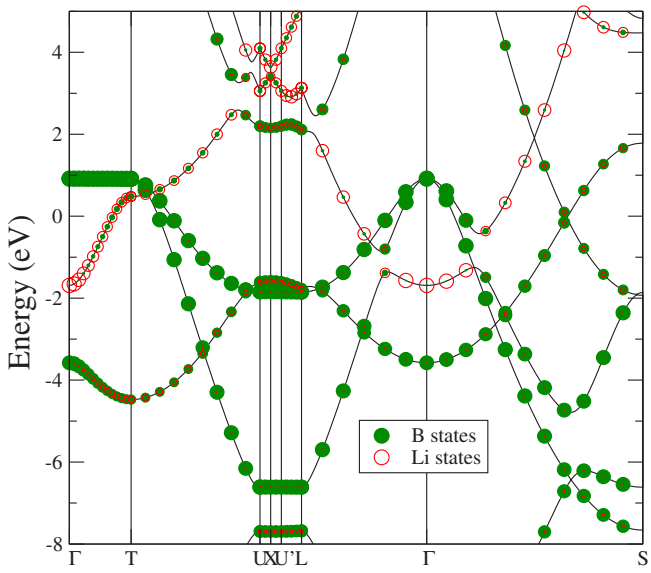

FIG. 1. (Color online) Band structure of LiB. The size of the empty (full) dots represents the amount of Li (B) character at a given **k** point. See Ref. 35 for high-symmetry points notation.

The pressure- and doping-induced changes in the electronic properties of LiB are studied with Vienna Ab initio Simulation Package (VASP)[32,33] within the GGA.[29] We use projector augmented waves[34] (PAW) pseudopotentials, in which Li semicore states are treated as valence; the energy cutoff is set at 30 Ryd. The projected electronic density of states (EDOS) is found by decomposition of the wave function within a sphere of the default PAW radius of 1.7 a.u. For the MS1 unit cell, the $2\times2\times3$-MS1 and $2\times2\times1$-MS2 supercells we use $31\times31\times31$, $18\times18\times6$, and $18\times18\times10$ Monkhorst-Pack **k** meshes, respectively.

III. BAND-STRUCTURE, DOS AND FERMI SURFACE

The band structure of LiB is presented in Fig. 1 (see Ref. 35 for high-symmetry points notation). Similarly to what happens in MgB_2,[2] there are two boron σ bands crossing the Fermi energy ϵ_F. Compared to the σ bands in MgB_2, these bands are even more two dimensional (due to the larger interlayer distance) and shifted by more than 0.6 eV to higher energies at the Γ point. As in MgB_2, they generate two cylindrical Fermi surfaces (in our case with axes along the ΓT direction, Fig. 2). The boron π states in LiB resemble more the π states of graphite, as they cross exactly at ϵ_F, so that LiB is lacking π Fermi surfaces altogether. In MgB_2 these states cross at about 2 eV above ϵ_F, which leads to the appearance of an extended π Fermi surface.[4] Another impor-

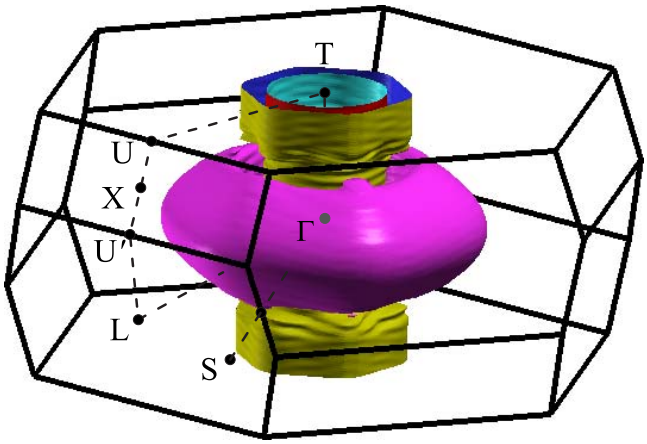

FIG. 2. (Color online) Fermi surface of MS1-LiB. For convenience, the Brillouin zone is stretched along the z direction.

tant difference between the electronic structures of the two borides is the presence of a lithium band at ϵ_F in LiB. The position of this band resembles the intercalant band in CaC_6,[13] although in LiB it has substantial hybridization to boron states close to the T point. The corresponding Fermi surface (a compressed sphere) is depicted in Fig. 2.

The total density of states (EDOS) and the EDOS projected over atomic orbitals is illustrated in Fig. 3. The main component at ϵ_F is given by boron $p\sigma$ states. As in graphite the boron $p\pi$ EDOS at ϵ_F is zero and increases slowly and linearly immediately after ϵ_F.

IV. PHONON SPECTRUM AND SUPERCONDUCTING PROPERTIES

The phonon dispersion and the phonon density of states (PHDOS) are illustrated in Fig. 4. The phonon modes at the Γ point are decomposed as $2A_{1g}+2A_{2u}+2E_g+2E_u$.[36] To distinguish between modes with the same symmetry but different eigenvectors we use the following notation: $A_{1g}[B_z]$,

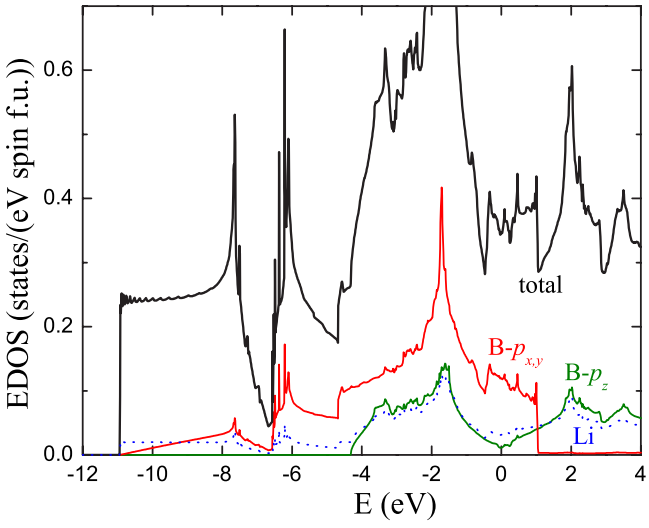

FIG. 3. (Color online) Electronic density of states projected over selected atomic orbitals.

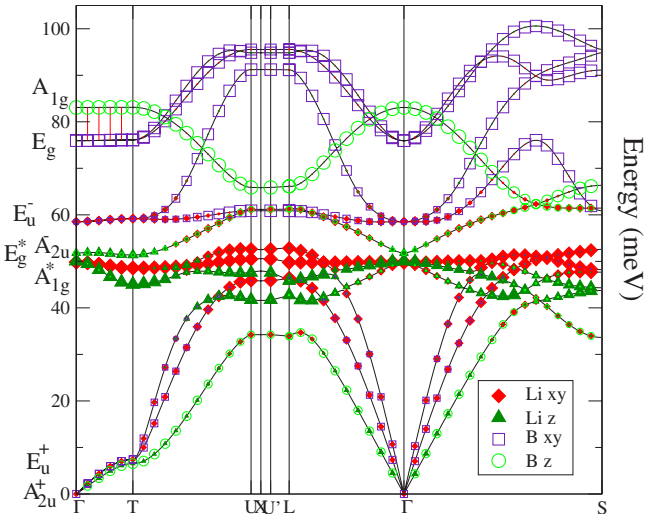

FIG. 4. (Color online) Phonon dispersion of MS1-LiB with decomposition into in-plane Li and B vibrations (labeled Li_{xy} and B_{xy}, respectively) and out-of-plane Li and B vibrations (labeled Li_z and B_z, respectively). Notation for the phonon modes at the Γ point, given next to the vertical axis, is explained in the text.

$E_g[B_{xy}]$, $E_u^-[(Li-B)_{xy}]$, $A_{1g}^*[Li_z]$, $A_{2u}^-[(Li-B)_z]$, $E_g^*[Li_{xy}]$, $A_{2u}^+[(Li+B)_z]$, $E_u^+[(Li+B)_{xy}]$, where in brackets we give the corresponding atoms and vibrations. For convenience, we label phonon branches everywhere in the Brillouin zone using the name of their representation at Γ.

Except for acoustic modes, a clear separation exists between optical Li and B vibrations. Li modes are confined in the 40–55 meV region and are not dispersive, meaning that Li-vibrations behave essentially as Einstein modes. Boron in-plane vibrations are softened along the ΓT direction due to coupling to the σ bands. The softening at Γ of the E_g phonon branches is approximately ~20 meV, to be compared with the 25~30 meV in MgB_2 for the E_{2g} modes.[5,37,38] This suggests a strong coupling of the σ bands to the in-plane vibrations in LiB,[25] almost as strong (or comparable) to that of MgB_2.

The three acoustic modes along the ΓT direction are substantially softer with respect to the other directions. At the zone border, T, these modes are formed by (i) in-plane $(Li+B)_{xy}$ vibrations at energies ≈8.5 meV and (ii) out-of-plane $(Li+B)_z$ vibrations at ≈8.0 meV. They can be related to the soft modes at the Γ point in MS2-LiB, discussed in Ref. 25.

The superconducting properties can be understood calculating the electron-phonon coupling $\lambda_{\mathbf{q}\nu}$ for a phonon mode ν with momentum $\mathbf{q}$:

$$\lambda_{\mathbf{q}\nu} = \frac{4}{\omega_{\mathbf{q}\nu} N(0) N_k} \sum_{\mathbf{k},n,m} |g^{\nu}_{\mathbf{k}n,\mathbf{k}+\mathbf{q}m}|^2 \delta(\epsilon_{\mathbf{k}n}) \delta(\epsilon_{\mathbf{k}+\mathbf{q}m}), \quad (1)$$

where the sum is over the Brillouin zone. The matrix element is $g^{\nu}_{\mathbf{k}n,\mathbf{k}+qm} = \langle \mathbf{k}n | \delta V / \delta u_{\mathbf{q}\nu} | \mathbf{k}+\mathbf{q}m \rangle / \sqrt{2\omega_{\mathbf{q}\nu}}$, where $u_{\mathbf{q}\nu}$ is the amplitude of the displacement of the phonon, V is the Kohn-Sham potential, and $N(0)$ is the electronic density of states at the Fermi level. The calculated average electron-phonon coupling is $\lambda = \Sigma_{\mathbf{q}\nu} \lambda_{\mathbf{q}\nu} / N_q \approx 0.62$ (N_k and N_q are the previously

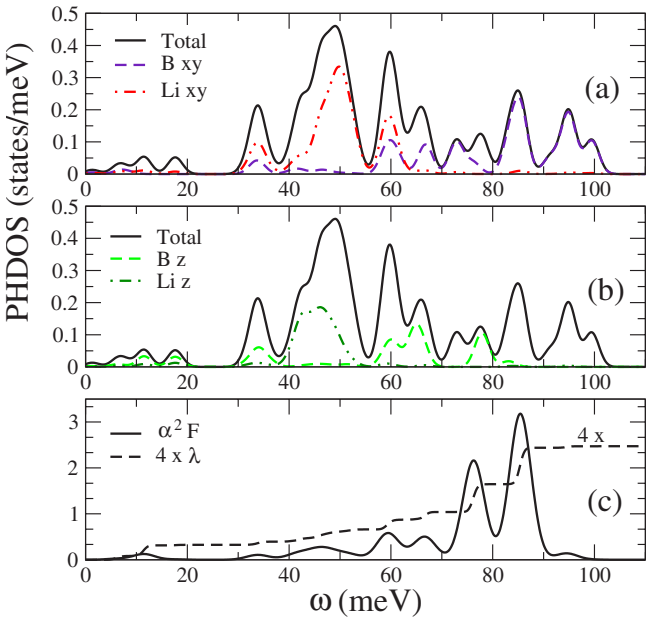

FIG. 5. (Color online) Phonon density of states (PHDOS), partial phonon density of states projected over selected vibrations, Eliashberg function, and integrated Eliashberg function for MS1-LiB. For clarity, the integrated Eliashberg function has been multiplied by a factor of 4.

defined **k**-space and **q**-space mesh dimensions, respectively).

The Eliashberg function

$$\alpha^2 F(\omega) = \frac{1}{2N_q} \sum_{\mathbf{q}\nu} \lambda_{\mathbf{q}\nu} \omega_{\mathbf{q}\nu} \delta(\omega - \omega_{\mathbf{q}\nu}) \tag{2}$$

and the integral $\lambda(\omega) = 2\int_0^\omega d\omega' \alpha^2 F(\omega')/\omega'$ are shown in Fig. 5. As can be seen most of the contribution comes from phonon states in the 60–90 meV region and a smaller contribution comes from low energy states.

An estimate of the different contributions of the in-plane (Li_{xy} and B_{xy}) and out-of-plane (Li_z and B_z) vibrations to λ can be obtained from the relation

$$\lambda = \sum_{i\alpha j\beta} \Lambda_{i\alpha,j\beta} = \sum_{i\alpha j\beta} \frac{1}{N_q} \sum_{\mathbf{q}} [\mathbf{G}_\mathbf{q}]_{i\alpha,j\beta} [\mathbf{C}_\mathbf{q}^{-1}]_{j\beta,i\alpha}, \tag{3}$$

where i,α indices indicate the displacement of the ith atom in the Cartesian direction α, $[\mathbf{G}_\mathbf{q}]_{i\alpha,j\beta} = \Sigma_{\mathbf{k},n,m} 4\tilde{g}^*_{i\alpha}\tilde{g}_{j\beta}\delta(\epsilon_{\mathbf{k}n})\delta(\epsilon_{\mathbf{k}+\mathbf{q}m})/[N(0)N_k]$, and $\tilde{g}_{i\alpha} = \langle \mathbf{k}n|\delta V/\delta x_{\mathbf{q}i\alpha}|\mathbf{k}+\mathbf{q}m\rangle/\sqrt{2}$. The $\mathbf{C}_\mathbf{q}$ matrix is the Fourier transform of the force constant matrix (the derivative of the forces with respect to the atomic displacements). The decomposition leads to

$$\mathbf{\Lambda} = \begin{array}{c} \\ \mathrm{B}_{xy} \\ \mathrm{B}_z \\ \mathrm{Li}_{xy} \\ \mathrm{Li}_z \end{array} \begin{array}{c} \begin{array}{cccc} \mathrm{B}_{xy} & \mathrm{B}_z & \mathrm{Li}_{xy} & \mathrm{Li}_z \end{array} \\ \begin{pmatrix} 0.46 & 0.00 & -0.02 & 0.00 \\ 0.00 & 0.13 & 0.02 & -0.05 \\ -0.02 & 0.02 & 0.08 & -0.01 \\ 0.00 & -0.05 & -0.01 & 0.07 \end{pmatrix} \end{array}. \tag{4}$$

The off-diagonal terms are small (but not negligible) compared to the total λ. Most of the coupling is to the in-plane B vibration; contributions from the Li and the out-of-plane B vibrations are smaller. Since the σ bands do not couple to the B_z vibrations and since there are no π Fermi surfaces, the coupling to B_z vibrations is due to the intercalant band. Note that the decomposed values of λ contain contributions from different modes and are summed over all the **q** points in the Brillouin zone. For example, $\Lambda_{\mathrm{B}_{xy},\mathrm{B}_{xy}} = 0.46$ includes the coupling to the in-plane E_g, E_u^-, and E_u^+ branches. By examining the integrated Eliashberg function $\lambda(\omega)$ in Fig. 5(c) and the phonon characters in Fig. 4 one can infer that the E_g branch is the most important of the three: among them it has the highest PHDOS in the 70–100 meV range, in which λ gains most of its total value. The soft in-plane E_u^+ branch is far less important, as the net contribution from all the soft modes having energy under 20 meV is only ≈0.08 [Fig. 5(c)].

It is instructive to compare our result with other layered superconductors. In MgB_2 the coupling of the σ bands to the phonon modes is $\lambda_\sigma^{\mathrm{MgB}_2} = 0.62 \pm 0.05$,[5] while in LiB the corresponding value is less than 0.46, as discussed above. This difference can be clarified by noting that the E_{2g} phonon linewidth $\gamma_{\mathbf{q},E_{2g}} = 2\pi N(0)\omega^2_{\mathbf{q}E_{2g}}\lambda_{\mathbf{q}\nu}$ along ΓA in MgB_2 happens to be comparable in magnitude with that of the E_g mode along ΓT in LiB. Therefore, the reduced electron-phonon coupling in LiB is mainly due to the E_g phonon frequency being harder than the E_{2g} one in MgB_2 [$\omega_{E_g}^{\mathrm{LiB}}/\omega_{E_{2g}}^{\mathrm{MgB}_2} \approx 1.2$ at Γ (Ref. 38)]. This unfortunate result can be linked to the absence of the π carriers, which play an important role in softening of the E_{2g} mode in MgB_2,[39,40] or to the slightly shorter bond length (the bond length shortening could be the result of the different level of B doping, different redistribution of the charge between the σ and π states, different ions or all of the above).

We find that LiB and graphite intercalated compounds have few similarities in terms of superconducting features. In particular, in CaC_6 the intercalant modes are responsible of ~50% of the total electron-phonon coupling, and the rest comes from vibrations of carbon modes in the direction perpendicular to the graphite layers. In CaC_6 one has $\lambda_{\mathrm{Ca}_{xy}} + \lambda_{\mathrm{Ca}_z} = 0.33$ and $\lambda_{\mathrm{C}_z} = 0.33$.[13] In LiB the overall contribution of B_z, Li_{xy}, and Li_z vibrations is less than half of that of CaC_6, which means that while LiB captures some of the physics of MgB_2, it does not capture the physics of graphite intercalated compounds to full extent. This is also clear from the phonon spectrum of CaC_6 where the intercalant modes are at energies lower than 20 meV and one of the Ca modes undergoes a marked softening with a corresponding large electron-phonon coupling (at point X of Fig. 2 in Ref. 13). In LiB, on the contrary, the Li modes are much higher in energies (~50 meV) meV and dispersionless. The main reason for this difference comes from the mass of Li which is 5.77 times smaller than that of Ca leading to frequencies which are on average 2.4 times larger.

The critical superconducting temperature is estimated using the McMillan formula[41]

$$T_c = \frac{\langle\omega\rangle_{\log}}{1.2} \exp\left[-\frac{1.04(1+\lambda)}{\lambda - \mu^*(1+0.62\lambda)}\right], \tag{5}$$

where μ^* is the screened Coulomb pseudopotential and

$$\langle\omega\rangle_{\log} = \exp\left[(2/\lambda) \int_0^{+\infty} \alpha^2 F(\omega) \ln(\omega)/\omega d\omega \right] \quad (6)$$

the phonon frequencies logarithmic average. We obtain $\langle\omega\rangle_{\log}=54$ meV leading to T_c of approximately 10–15 K for $\mu^*=0.14-0.10$. This value could be further enhanced by multiband effects.

V. DOPING AND PRESSURE EFFECTS

Even though a theoretically-devised from scratch superconductor with $T_c=10-15$ K could be considered a success of the materials prediction methodology, the stoichiometric LiB compound falls short of expectations to compete with the record-holding binary MgB_2. In this section we investigate whether it is possible to favorably modify the electronic properties of LiB and achieve higher T_c by doping or applying pressure. We pay special attention to the evolution of the π states, since their reintroduction at ϵ_F may soften the E_g mode and lead to a larger coupling.

As has been pointed out previously,[25] the bonding π states are completely filled under ambient conditions. Because the band crossing in LiB at the Fermi level is accidental, it may be possible to move the crossing point with pressure and increase the π-band EDOS at ϵ_F. Figure 6(a) reveals that there is indeed a rapid change in the σ and π EDOS, followed by a plateau after 5 GPa. This behavior is a reflection of two distinctly different regimes of the LiB structural changes: (i) in the 0–5-GPa pressure range the Li-Li interlayer spacing quickly shrinks and the B-B bond length slightly expands so that at 5 GPa they become about 0.5 and 1.02 of their zero-pressure values, respectively; (ii) for pressures above 5 GPa the Li atoms in the bilayer start experiencing the hard-core repulsion and the compound compresses more isotropically. The inset in Fig. 6(a) illustrates that by reducing the Li-Li interlayer distance one forces the charge from the intercalant band (completely emptied at about 6 GPa) into the boron π and σ states (lowered by 0.7 eV at that pressure). Once the charge redistribution is complete, no appreciable changes in the EDOS are seen for the boron states up to at least 30 GPa. Therefore, the peculiar behavior of the nearly free electron intercalant states (also observed in other systems[12,42,43]) is the only meaningful factor allowing modification of the LiB boron states with pressure.

These simulations demonstrate that the compression of LiB does not lead to the desired π-band EDOS values comparable to those in MgB_2. Moreover, the hydrostatic pressure causes such a quick drop in the σ-band EDOS that this will likely negate any possible enhancement in the electron-phonon coupling due to the reintroduction of the π states at ϵ_F. The phonon modes are also expected to harden under pressure, further reducing the electron-phonon coupling in LiB.[44]

LiB has plenty of available bonding σ states, therefore the compound should be easy to electron dope. A quick examination of the boron EDOS states around the Fermi level (Fig. 3 or 4 in Ref. 25) gives an idea on what possible changes in the Fermi surfaces and, eventually, in the electron-phonon

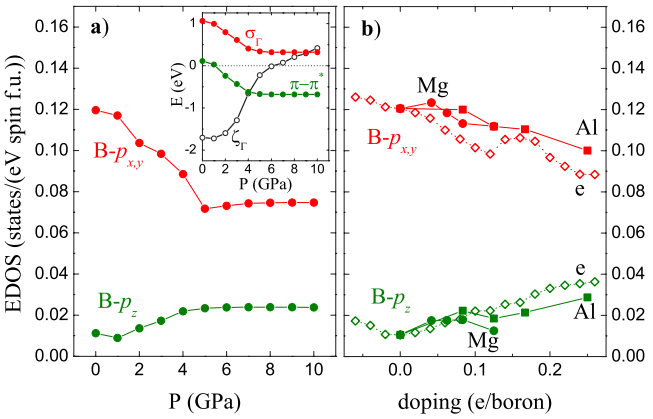

FIG. 6. (Color online) (a) EDOS at the Fermi level projected over σ and π states as a function of pressure; (b) the same as a function of doping level: the hollow points represent charged LiB unit cell in a neutralizing background; the solid points correspond to substitutional Mg and Al doping of LiB in the MS1 and MS2 superstructures described in the text (Ref. 45). For comparison, the σ and π EDOS in MgB_2 are 0.098 and 0.064 states/(eV spin f.u.), respectively. The inset shows pressure-induced changes in the position of different states near the Fermi level: σ-boron and intercalant (labeled ζ) states at the Γ point and crossing of the π-π^* states along the ΓS direction.

coupling the doping could lead to. At small doping levels, when the rigid band approximation normally holds, the EDOS from the two dimensional σ bands should only slightly fluctuate until the states are completely filled, which happens at $\Delta q \approx eN(0)\Delta E \approx 0.70$ $(e/\text{eV})\cdot(1$ eV$)$ $=0.70$ e/f.u.$=0.35$ e/boron. The EDOS from the π bands grows slowly and even at the relatively high electron doping of 0.35 e/boron it would amount only to about a half of what is observed in MgB_2. Another way to tweak the electronic structure could be to hole-dope LiB as it is done for Li_xBC.[18,19] The known limitations of this approach are the buckling of the hexagonal layers and the eventual destabilization of the compound upon heavy Li depletion.[18,19]

We first simulate the electron (hole) doping using a charged cell with a neutralizing positive (negative) background. Normally, in this approach one can safely relax the unit cell parameters and obtain valuable information about the bond length variation under small doping. However, in the case of the electron-doped LiB the repulsion between the negatively charged boron layers overcomes the weak binding between the lithium layers, causing the c axis to undergo unphysical expansion even at small levels of doping. Therefore, we fix the c axis at the zero-doping value and relax only the remaining three parameters. The set of data, shown as hollow points in Fig. 6(b), supports our earlier conclusion that the π band EDOS cannot be easily increased. Note that the approximations used in this test, i.e., the fixed c axis and the use of a neutralizing background, may influence the results to some extent. For example, the positive electrostatic potential from ionized dopants could bring the delocalized π states down (in addition to the rigid band downshift) and could potentially be an important factor in increasing the π EDOS.

To address these limitations we use a more realistic model of the electron-doped LiB by substituting Li with Mg or Al.

Small doping levels are obtained only for large unit cells; we use the hexagonal $2\times2\times3$-MS1 and $2\times2\times1$-MS2 supercells with 48 and 32 atoms, respectively. Replacement of one or two Li atoms in these structures results in the 1/24, 1/16, 1/12, and 1/8 concentrations of dopants per boron, and the level of doping is found in the assumption that they give up all their valence charge. In all the cases the c-axis expansion in the fully relaxed unit cells does not exceed 6%. The resulting averaged boron EDOS for the Mg and Al sets are shown in Fig. 6(b) as solid points.[45] The scattered presence of dopants in the lattice should cause some dispersion of the local boron properties. A general trend observed in our supercell calculations is that a downshift of the π and σ states happens only for B layers in direct contact with the dopant. Typical values of the downshift that a single Mg (Al) atom induces in all eight atoms in a neighboring B layer are about 0.2 (0.5) eV. It is not easy to isolate the importance of different factors defining the level of B doping, i.e., the simple charge transfer, the electrostatic effect discussed above and the structural changes. However, Fig. 6(b) demonstrates that the net effect of the substitutional doping is described reasonably well within the rigid band model.

In summary, our tests indicate that it is rather difficult to reintroduce a significant amount of π states at ϵ_F with hydrostatic pressure or small doping, because the band crossing in LiB happens to be exactly at ϵ_F, about 2 eV lower than in MgB_2. To have a chance of substantially increasing T_c, one should search for more radical ways of modifying the electronic structure of the MS metal borides.

VI. CONCLUSIONS AND PERSPECTIVES

In this work we have investigated electron and phonon properties of the recently theoretically devised superconductor LiB.[25] By studying in details the phonon properties of this hypothetical material we have found that its critical temperature is of the order of 10–15 K. Superconductivity is mainly of the MgB_2 kind with planar $p\sigma$ bands strongly coupled with phonons. Differently from MgB_2, LiB has no Fermi surface generated by π states but an additional intercalant one. Thus, its electronic structure can be seen as a hybrid between MgB_2 and CaC_6. However, the intercalant electronic states of LiB are weakly coupled with the Li and B_z vibrations so that the overall electron-phonon coupling is only $\lambda=0.62$.

Since the discovery of MgB_2, no other diborides have been found with high T_c (for a full list, see Ref. 46). If we compare LiB with the known diborides, our calculated 10–15 K critical temperature is not so low, although it is far from the 39 K of MgB_2. Nevertheless, the study of LiB gives an important understanding. The common belief is that the main effect for the singular and unique behavior of MgB_2 is given by the presence of almost two-dimensional σ bands. LiB has even more planar σ bands and even higher σ EDOS at ϵ_F relative to that in MgB_2;[25,26] however, their contribution to the total electron-phonon coupling turns out to be at least 25% smaller. This reduction can be attributed to the differences between the in-plane boron vibrations in the two borides, caused mainly by the lack of the π carriers at ϵ_F in LiB. Namely, the softening of the E_g mode in LiB is smaller compared to that of E_{2g} in MgB_2, which is one of the factors making the former mode harder ($\omega_{E_g}^{\mathrm{LiB}}/\omega_{E_{2g}}^{\mathrm{MgB_2}}\approx1.2$ at Γ). Therefore, in addition to the direct loss of the π states contribution to λ, their absence at ϵ_F in LiB also has a strong indirect negative effect on the overall electron-phonon coupling.

We have investigated whether this somewhat unexpected obstacle, preventing LiB to be a truly high-T_c superconductor, could be overcome with moderate modifications of the compound's properties. Behavior of electronic features important for the LiB superconductivity has been examined as a function of small doping and pressure. Our results indicate that the π EDOS increases very slowly and cannot reach the desired values, at least not before the σ EDOS is substantially reduced. Thus, small doping and pressure are not expected to significantly improve T_c in LiB. A promising direction to fix the problem would be to find a suitable LiB-based ternary alloy; this question is currently under investigation.

Theoretical development of potentially important superconducting materials is a difficult task because T_c critically depends on their band structure features and vibrational properties. The challenge is even greater if one attempts to design a superconductor from scratch, since one first needs to ensure its thermodynamic stability. The case of LiB shows that it is possible to theoretically predict a compound that both (i) has a good chance to form and (ii) possesses interesting superconducting properties. Study of such promising candidates gives important insight into how to perform a more targeted search for novel superconducting materials.

Recently, a preprint on the related structure MS2-LiB appeared on-line.[40] The results of the paper are similar to ours except for some numerical details that can probably be related to the different unit cells and $\mathbf{k},\mathbf{q}$-point samplings used.[47] However, our conclusions concerning the possibility of increasing the T_c in LiB by doping are rather different, as explained in the previous section.

ACKNOWLEDGMENTS

We acknowledge many fruitful discussions with Igor Mazin, Francesco Mauri, Michele Lazzeri, and Roxana Margine. Calculations were performed at the San Diego Supercomputing Center (MCA06N039) and at IDRIS supercomputing center (Project No. 061202). This research was partially supported by ONR.

[1] J. Nagamatsu, N. Nakagawa, T. Muranaka, Y. Zenitani, and J. Akimitsu, Nature (London) **410**, 63 (2001).
[2] J. M. An and W. E. Pickett, Phys. Rev. Lett. **86**, 4366 (2001).
[3] K. D. Belashchenko, M. van Schilfgaarde, and V. P. Antropov, Phys. Rev. B **64**, 092503 (2001).
[4] J. Kortus, I. I. Mazin, K. D. Belashchenko, V. P. Antropov, and L. L. Boyer, Phys. Rev. Lett. **86**, 4656 (2001).
[5] Y. Kong, O. V. Dolgov, O. Jepsen, and O. K. Andersen, Phys. Rev. B **64**, 020501(R) (2001).
[6] A. S. Cooper, E. Corenzwit, L. D. Longinotti, B. T. Matthias, and W. H. Zachariasen, Proc. Natl. Acad. Sci. U.S.A. **67**, 313 (1970).
[7] V. A. Gasparov, N. S. Sidorov, I. I. Zverkova, and M. P. Kulakov, arXiv:cond-mat/0102421 (unpublished).
[8] L. Leyvarovska and E. Leyvarovski, J. Less-Common Met. **67**, 249 (1979).
[9] T. E. Weller, M. Ellerby, S. S. Saxena, R. P. Smith, and N. T. Skipper, Nat. Phys. **1**, 39 (2005).
[10] N. Emery, C. Herold, M. d'Astuto, V. Garcia, C. Bellin, J. F. Mareche, P. Lagrange, and G. Loupias, Phys. Rev. Lett. **95**, 087003 (2005).
[11] M. S. Dresselhaus and G. Dresselhaus, Adv. Phys. **51**, 1 (2002).
[12] G. Csányi, P. B. Littlewood, A. H. Nevidomskyy, C. J. Pickard, and B. D. Simons, Nat. Phys. **1**, 42 (2005).
[13] M. Calandra and F. Mauri, Phys. Rev. Lett. **95**, 237002 (2005).
[14] I. I. Mazin, Phys. Rev. Lett. **95**, 227001 (2005).
[15] M. Calandra and F. Mauri, Phys. Rev. B **74**, 094507 (2006).
[16] A. Gauzzi, S. Takashima, N. Takeshita, C. Terakura, H. Takagi, N. Emery, C. Herold, P. Lagrange, and G. Loupias, arXiv:cond-mat/0603443 (unpublished).
[17] H. Rosner, A. Kitaigorodsky, and W. E. Pickett, Phys. Rev. Lett. **88**, 127001 (2002).
[18] A. M. Fogg, J. B. Claridge, G. R. Darling, and M. J. Rosseinsky, Chem. Commun. (Cambridge) **12**, 1348 (2003).
[19] A. M. Fogg, J. Meldrum, G. R. Darling, J. B. Claridge, and M. J. Rosseinsky, J. Am. Chem. Soc. **128**, 10043 (2006).
[20] D. de Fontaine, in *Solid State Physics*, edited by H. Ehrenreich and D. Turnbull (Academic Press, New York, 1994), Vol. 47, pp. 33–176.
[21] G. Ceder, Comput. Mater. Sci. **1**, 144 (1993).
[22] S. Curtarolo, D. Morgan, K. Persson, J. Rodgers, and G. Ceder, Phys. Rev. Lett. **91**, 135503 (2003).
[23] D. Morgan, G. Ceder, and S. Curtarolo, Meas. Sci. Technol. **16**, 296 (2005).
[24] S. Curtarolo, D. Morgan, and G. Ceder, CALPHAD: Comput. Coupling Phase Diagrams Thermochem. **29**, 163 (2005).
[25] A. N. Kolmogorov and S. Curtarolo, Phys. Rev. B **73**, 180501(R) (2006).
[26] A. N. Kolmogorov and S. Curtarolo, Phys. Rev. B **74**, 224507 (2006).
[27] For example, the long-period shifts have little effect on the MS-LiB energy: MS1 and MS2 have been demonstrated to be nearly degenerate under ambient conditions, so that the synthesized lithium monoboride could be a mixture of the two crystal structure phases (Ref. 25).
[28] http://www.pwscf.org, S. Baroni, S. de Gironcoli, A. Dal Corso, and P. Giannozzi, Rev. Mod. Phys. **73**, 515 (2001).
[29] J. P. Perdew, K. Burke, and M. Ernzerhof, Phys. Rev. Lett. **77**, 3865 (1996).
[30] N. Troullier and J. L. Martins, Phys. Rev. B **43**, 1993 (1991).
[31] S. G. Louie, S. Froyen, and M. L. Cohen, Phys. Rev. B **26**, 1738 (1982).
[32] G. Kresse and J. Hafner, Phys. Rev. B **47**, 558 (1993).
[33] G. Kresse and J. Furthmuller, Phys. Rev. B **54**, 11169 (1996).
[34] P. E. Blochl, Phys. Rev. B **50**, 17953 (1994).
[35] The special points are $\Gamma=(0,0,0)$, $T=(1/2,1/2,1/2)$, $U=(1/2+\eta,\tau,\tau)$, $X=(1/2,0,0)$, $U'=(1/2-\eta,-\tau,-\tau)$, $L=(1/4,-1/4,-1/4)$, $S=(1/2,-1/2,0)$. Given the rhombohedral angle α, the parameters η and τ are expressed as $\eta=\{1-2/[3\tan^2(\alpha/2)-1]\}/12$ and $\tau=\{1+1/[3\tan^2(\alpha/2)-1]\}/12$.
[36] D. L. Rousseau, R. P. Bauman, and S. P. S. Porto, J. Raman Spectrosc. **10**, 253 (1981).
[37] A. Shukla, M. Calandra, M. d'Astuto, M. Lazzeri, F. Mauri, C. Bellin, M. Krisch, J. Karpinski, S. M. Kazakov, J. Jun, D. Daghero, and K. Parlinski, Phys. Rev. Lett. **90**, 095506 (2003).
[38] We take the reference phonon frequency for the E_{2g} mode in MgB_2 as $\omega\sim 64$ meV at Γ and ~ 90 meV at M (Ref. 37).
[39] I. I. Mazin and V. P. Antropov, Physica C **385**, 49 (2003).
[40] A. Y. Liu and I. I. Mazin, Phys. Rev. B **75**, 064510 (2007).
[41] W. L. McMillan, Phys. Rev. **167**, 331 (1968).
[42] E. R. Margine and V. H. Crespi, Phys. Rev. Lett. **96**, 196803 (2006).
[43] J. S. Kim, L. Boeri, R. K. Kremer, and F. S. Razavi, Phys. Rev. B **74**, 214513 (2006).
[44] We do not observe any significant softening of the in-plane boron phonon mode resulting from the $\sim 2\%$ expansion of the boron-boron bond under small (below 5 GPa) pressures. The frequencies of the soft sliding modes have been shown to nearly double at 2 GPa (Ref. 25).
[45] We place the dopants in the supercell as uniformly as possible. Due to the high sensitivity of the projected EDOS to k sampling we use a 0.2 eV smearing in the MS1 and MS2 supercell calculations.
[46] C. Buzea and T. Yamashita, Semicond. Sci. Technol. **14**, R115 (2001).
[47] In compounds such as MgB_2, $\lambda_{\mathbf{q}\nu}$ varies substantially all over the Brillouin zone. Thus a better $\mathbf{q}$ point sampling than that possible in state-of-the-art *ab initio* simulations is needed to obtain estimates of λ comparable with that achieved for simple superconductors such as Nb. For this reason, in systems such as MgB_2, the errors in parameters such as λ or $\omega_{\log}$ is probably larger than expected.